JOURNAL OF THE ROYAL SOCIETY Interface

J. R. Soc. Interface (2010) **7**, 259–269
doi:10.1098/rsif.2009.0133
Published online 3 June 2009

Rate-dependent frictional adhesion in natural and synthetic gecko setae

Nick Gravish[1], Matt Wilkinson[1], Simon Sponberg[2], Aaron Parness[3], Noe Esparza[3], Daniel Soto[4], Tetsuo Yamaguchi[5,†], Michael Broide[6], Mark Cutkosky[3], Costantino Creton[4] and Kellar Autumn[1,*]

[1]*Department of Biology, and* [6]*Department of Physics, Lewis & Clark College, Portland, OR, USA*
[2]*Department of Integrative Biology, University of California, Berkeley, CA, USA*
[3]*Department of Mechanical Engineering, and* [4]*Department of Applied Physics, Stanford University, Stanford, CA, USA*
[5]*Laboratoire PPMD, ESPCI-CNRS-UPMC, Paris, France*

Geckos owe their remarkable stickiness to millions of dry, hard setae on their toes. In this study, we discovered that gecko setae stick more strongly the faster they slide, and do not wear out after 30 000 cycles. This is surprising because friction between dry, hard, macroscopic materials typically decreases at the onset of sliding, and as velocity increases, friction continues to decrease because of a reduction in the number of interfacial contacts, due in part to wear. Gecko setae did not exhibit the decrease in adhesion or friction characteristic of a transition from static to kinetic contact mechanics. Instead, friction and adhesion forces increased at the onset of sliding and continued to increase with shear speed from 500 nm s^{-1} to 158 mm s^{-1}. To explain how apparently fluid-like, wear-free dynamic friction and adhesion occur macroscopically in a dry, hard solid, we proposed a model based on a population of nanoscopic stick–slip events. In the model, contact elements are either in static contact or in the process of slipping to a new static contact. If stick–slip events are uncorrelated, the model further predicted that contact forces should increase to a critical velocity (V^*) and then decrease at velocities greater than V^*. We hypothesized that, like natural gecko setae, but unlike any conventional adhesive, gecko-like synthetic adhesives (GSAs) could adhere while sliding. To test the generality of our results and the validity of our model, we fabricated a GSA using a hard silicone polymer. While sliding, the GSA exhibited steady-state adhesion and velocity dependence similar to that of gecko setae. Observations at the interface indicated that macroscopically smooth sliding of the GSA emerged from randomly occurring stick–slip events in the population of flexible fibrils, confirming our model predictions.

Keywords: gecko adhesion; friction; tribology; adhesives

1. INTRODUCTION

Geckos are the world's supreme climbers, capable of attaching and detaching their adhesive toes in milliseconds while running with reckless abandon on vertical and inverted surfaces (Autumn 2006). Over two millennia ago, Aristotle commented on the ability of geckos to 'run up and down a tree in any way' (Aristotle 350 BCE 1918). We know now that it is the micro- and nanostructures on their toes that enable geckos' exceptional climbing performance (Maderson 1964; Russell 1975; Pianka & Sweet 2005; Autumn 2006). Gecko toes bear arrays of millions of angled, branched, hair-like setae (110 μm long by 2.1 μm radius) formed of stiff, hydrophobic β-keratin (elastic modulus, $E = 1.5$ GPa; Alibardi 2003; Autumn *et al.* 2006*c*; Rizzo *et al.* 2006; Peattie *et al.* 2007). Setae act as a bed of springs to conform to a variety of surface profiles (Persson 2003; Sitti & Fearing 2003; Autumn *et al.* 2006*c*). Each seta branches into a nanoarray of hundreds of smaller stalks (800 nm long, 25 nm radius) ending in thin spatular structures (200 nm wide, 5 nm thick) that make intimate contact with the substrate (Ruibal & Ernst 1965; Arzt *et al.* 2003; Huber *et al.* 2005*a*; Eimuller *et al.* 2008; Zhao *et al.* 2008).

While gecko setae can meet the challenges of dynamic climbing (Autumn *et al.* 2006*b*), and last for months under real-world conditions, conventional pressure-sensitive adhesives (PSAs) do not. PSAs, such as those of adhesive tapes, are fabricated from soft, viscoelastic materials (Pocius 2002; Creton 2003)

*Author for correspondence (autumn@lclark.edu).
†Present address: Department of Applied Physics, The University of Tokyo, Japan.

Electronic supplementary material is available at http://dx.doi.org/10.1098/rsif.2009.0133 or via http://rsif.royalsocietypublishing.org.

Received 6 April 2009
Accepted 6 May 2009

that (i) become dirty, (ii) self-adhere, (iii) attach accidentally to inappropriate surfaces, (iv) wear out, and (v) detach at the onset of sliding. In previous studies, we explained how gecko setae resist fouling by becoming cleaner with repeated use (Hansen & Autumn 2005; Hui *et al.* 2006; Lamb & Bauer 2006), and how a non-adhesive default state prevents self-adherence and inappropriate attachment (Autumn & Hansen 2006). This enabled the development of gecko-like synthetic adhesives (GSAs) with a non-adhesive default state (Lee *et al.* 2008; Qu *et al.* 2008; Schubert *et al.* 2008) and a self-cleaning function (Lee & Fearing 2008; Sethi *et al.* 2008). This study focuses on how the related phenomena of wear and sliding affect adhesion and friction in natural and synthetic gecko setae.

1.1. Kinetic friction and adhesion: why do geckos not fall when they slip?

Contact forces between dry solids (Bhushan 2002) typically decrease at the onset of sliding, and as velocity increases, force continues to decrease because of a reduction in the interfacial contact fraction, due in part to wear. This would represent an unstable dynamic condition for a climbing gecko: any slip would likely result in a fall (Autumn *et al.* 2006*a*). Yet, geckos do not fall when their feet slide (Huber *et al.* 2007; Jusufi *et al.* 2008). Indeed, gecko setae require shear displacement to initiate adhesion (Autumn *et al.* 2000, 2006*a*).

The application of a vertical preload (20–200 kPa), followed by a small drag in shear (5–10 μm; figure 1), brings the seta and its 100–1000 spatulae into sub-nanometre contact with the substrate (Autumn *et al.* 2000; Chen *et al.* 2008, 2009). Adhesion in gecko setae requires maintenance of a shear force (as described by the *frictional adhesion* model; Autumn & Hansen 2006; Autumn *et al.* 2006*a*; Tian *et al.* 2006). Force measurements over shear displacements from 20 to 500 μm in length showed that initially, frictional–adhesion forces increase linearly with shear displacement (Autumn *et al.* 2000; Gravish *et al.* 2007; Lee *et al.* 2008; Zhao *et al.* 2008), and approach steady-state values only after the setal tip begins to slide (approx. 5–10 μm) and reorient (Autumn *et al.* 2006*a*; Zhao *et al.* 2008) in the drag step (figure 1). Maximum friction and adhesion forces occur only after the onset of interfacial sliding (Autumn *et al.* 2007; Gravish *et al.* 2007; Lee *et al.* 2008; Zhao *et al.* 2008), suggestive of a viscous, fluid-like system (Bullock *et al.* 2008; Eimuller *et al.* 2008) but inconsistent with the well-documented rigid, dry structure of gecko setae (Ruibal & Ernst 1965; Russell 1975; Williams & Peterson 1982; Autumn *et al.* 2002, 2006*c*; Huber *et al.* 2005*b*, 2007; Rizzo *et al.* 2006; Peattie *et al.* 2007).

1.2. Rate dependence of contact forces

Friction is one of the most well-studied natural processes in the history of science (Bhushan 2002), yet only recently, with the inventions of the surface force apparatus (see Israelachvili (1992) for a review) and the atomic force microscope, have researchers begun to probe tribological processes at the nanoscale (Krim 1996). Relating macroscopic friction to the underlying nanoscale processes is challenging because of the complex dynamics of millions of single-asperity contacts between rubbing surfaces (Robbins & Smith 1996; Porto *et al.* 2000; Ringlein & Robbins 2004; Israelachvili 2005; Luan & Robbins 2005). Gecko adhesion has attracted considerable attention in surface science because it is a macroscopic system in which the contact

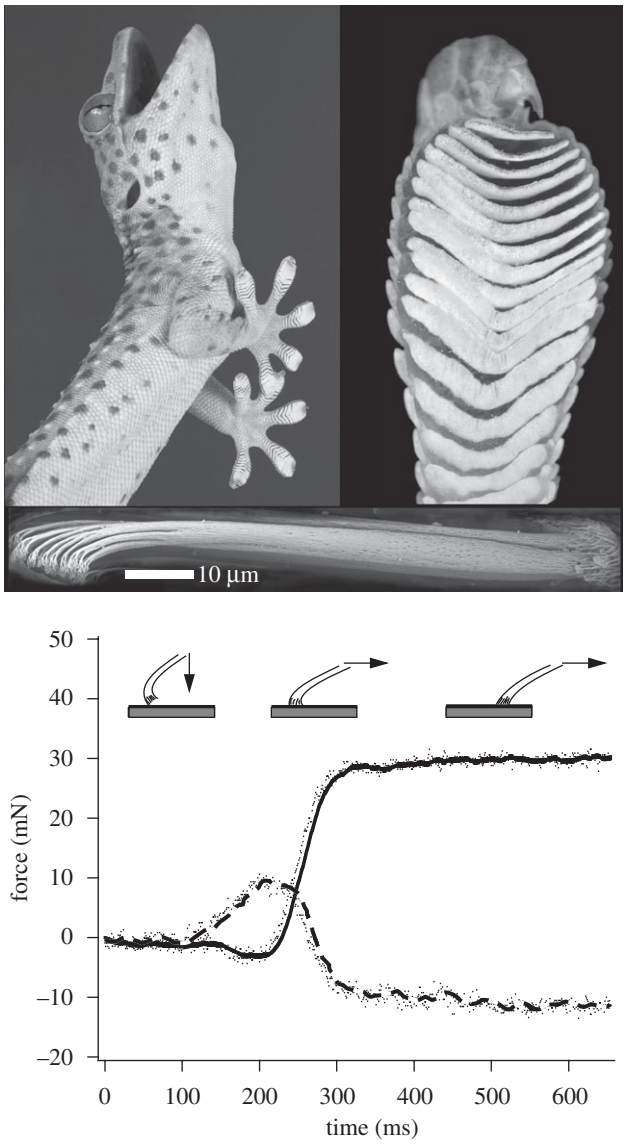

Figure 1. The tokay gecko (approx. 30 cm in length) possesses adhesive pads on the undersides of its toes (approx. 1 cm in length). Arrays of branched setae (approx. 110 μm in length) achieve intimate contact with surfaces to engage intermolecular van der Waals forces. Setae are adhesive only under the application of a shear force. Setae are first applied vertically to a surface and then sheared parallel to the surface. The setal shafts load elastically until the elastic component is saturated, at which point the setae slide across the substrate while remaining in adhesion. As the adhesive begins to slide (300 ms), friction and adhesion forces remain constant and do not exhibit any notable decrease, uncharacteristic of solid contact mechanics. The solid line represents friction and the dashed line adhesion. Note that for normal force, adhesion is negative while compression is positive.

mechanics are a consequence of well-defined nanoscopic geometry (Autumn *et al.* 2000; Huber *et al.* 2005*a*; Tian *et al.* 2006; Zhao *et al.* 2008).

Solid friction between multi-contact interfaces usually abides by the rate–state friction model (Rice & Ruina 1983; Baumberger *et al.* 1999) where contact time increases contact area (contact aging; Sills *et al.* 2007), and thus kinetic forces are typically smaller than static forces. However, theory suggests that branched gecko setae reduce the stress concentrations typically associated with fracture (Hui *et al.* 2004), and in fact setae attach well in both the static and kinetic regimes (Autumn *et al.* 2000, 2006*a*; Zhao *et al.* 2008). Synthetic setae may resist stress-induced wear through compliance and load-sharing (Bhushan *et al.* 2008). Stable and repeatable adhesion while sliding over distances thousands of times greater than the length of a single spatular bond (200 nm) implies the presence of non-trivial kinetic contact mechanics in the gecko adhesive.

We investigated friction and adhesion dynamics in isolated tokay gecko setal arrays by measuring contact forces over five orders of magnitude of shear velocity, and proposed a model based on a population of nanoscopic stick–slip events, explaining how wear resistance and viscous-like kinetic forces can occur at the macroscale in a dry, hard material. To test our model, we explored the dynamic response of a novel GSA.

2. METHODS

2.1. Samples and measurement

Setal arrays were gathered from live non-moulting tokay geckos (*Gekko gecko*) and mounted on scanning electron microscope stubs using Loctite 410 (Henkel Co., CT) as described previously (Autumn *et al.* 2002; Gravish *et al.* 2007). Prior to testing, the samples were inspected to ensure no wicking of glue occurred in the setal shafts.

The setal array test platform, RoboToe, has been described previously (Autumn *et al.* 2006*a*; Gravish *et al.* 2007). Mounted setal array samples were held in a specimen chuck attached to a Kistler 9328A three-axis piezoelectric force sensor (Kistler, Winterthur, Switzerland). The force sensor and sample were mounted atop a Newport RP Reliance breadboard table (Newport, Irvine, CA). New pre-cleaned slides (Erie Scientific, Portsmouth, NH) were cleaned in a bath of 2 M NaOH (Ted Pella, Redding, CA) for 15 min followed by a triple series of ultrapure deionized water rinses and Kimwipe dry (Kimberly-Clark, Neenah, WI) to ensure that the substrate was clean. Freshly cleaned slides were mounted on a two-axis nanopositioning system comprising two Aerotech ANT-50L (Aerotech, Pittsburgh, PA) linear actuators with maximum travel of 50 mm and velocities from 10 nm s^{-1} to 250 mm s^{-1}.

The resolution of the force sensor was 2.5 mN and the actuator resolution was 10 nm. The stiffness of the measurement system was approximately 320 N mm^{-1} (Autumn *et al.* 2006*c*), which is more than 30 times greater than the 1–10 N mm^{-1} average shear stiffness of setal arrays (Autumn *et al.* 2000; Gravish *et al.* 2007), and thus, considering the force sensor and setae in series, the elastic contribution from the measurement system is negligible. We aligned the sample and substrate surfaces to be coplanar using two Newport goniometers as well as a linear slope correction in software.

2.2. Rate dependence and wear resistance in gecko setae

We measured friction and adhesion forces at 12 different drag velocities over the velocity range of 500 nm s^{-1} to 158 mm s^{-1}. Due to temporal constraints on the length of individual tests, we had to run slower tests over smaller displacements and faster tests over larger displacements similar to the methods of Vorvolakos & Chaudhury (2003), Tambe & Bhushan (2005) and Tao & Bhushan (2007). We chose five drag distances (from 1 μm to 10 mm), each an order of magnitude larger than the last to test for velocity dependence. In all, 24 individual velocity and distance combinations were tested five times, totaling 120 tests per sample. In total, 25 setal arrays were subjected to 120 shear tests for a total of 3000 trials. However, as discussed in §3, 14 arrays survived the battery of tests undamaged, leaving 1680 of the 3000 trials in the analysis.

Approximately 70 μm tall setal arrays (Autumn *et al.* 2006*c*) were preloaded to a normal displacement of 35 μm. Normal displacement was measured from the point at which setal array and slide made first contact. Once preloaded, each test began with a 50 μm engagement drag at a constant velocity of 100 μm s^{-1}. Immediately following the engagement drag, the slide accelerated at 1500 mm s^{-2} to the predetermined velocity and dragged over the specified distance until completed. After completion of the velocity drag, arrays were unloaded at 45° until out of contact with the glass slide. Loading and unloading motions were performed at 500 μm s^{-1}. Perpendicular load–pull tests were conducted at the beginning and end of each test set to calculate array stiffness to identify (and discard) any arrays damaged during the experiments (Autumn *et al.* 2006*c*). To assess the wear resistance of setae, we subjected two samples to a battery of 30 000 load–drag–pull tests at a velocity of 10 mm s^{-1} over a distance of 10 mm per trial, totalling a net displacement of 300 m. We recorded friction, adhesion and sample stiffness in the normal direction every 1000 trials.

2.3. Fabrication of GSA

Since gecko spatulae are smaller than the wavelength of visible light, the details of the sliding mechanism for natural gecko setal arrays occur at a scale that is not accessible optically. To test the fibrillar stick–slip model, we explored the dynamic response of a GSA with dimensions greater than those of the natural gecko material. Because contact mechanics are controlled by a balance between (surface-dependent) adhesive energy and (volume-dependent) elastic energy, increasing the size of the system while maintaining a similar contact geometry requires a decrease in the

elastic modulus of the material. Our GSA comprised wedge-like fibrils 45 μm in width and 155 μm in height (approx. 3.5 : 1 aspect ratio; Santos 2009; Parness *et al.* in press), so we chose a polydimethylsiloxane elastomer (PDMS, Sylgard-170; $E = 1.75$ MPa) in proxy of hard keratin. We employed a lithographic process with two exposure angles to create moulds for the GSA out of a negative tone photoresist, SU-8 (Microchem.com). We cast the Sylgard elastomer in the SU-8 mould under vacuum, spun it down to the desired backing layer thickness of 155 μm, then heat cured it and pulled it out of the mould by hand.

2.4. Rate dependence and wear resistance in GSA

Taking into account the GSA's larger contact geometry, we conducted similar frictional–adhesion velocity and durability tests on the synthetic structure over an increased drag distance range from 100 μm to 30 mm and velocities from 5 μm s^{-1} to 158 mm s^{-1}. We recorded kinetic friction and adhesion forces at 13 drag distance/velocity combinations of nine trials each, totaling 117 tests. We subjected the synthetic adhesive to the same durability test as that performed on setal arrays: 30 000 load–drag–pull tests at a velocity of 10 mm s^{-1} over a distance of 10 mm per trial, totalling a net displacement of 300 m. We recorded friction, adhesion and sample stiffness in the normal direction every 1000 trials. Lastly, we recorded high-speed videos of the real-time contact area of the synthetic adhesive using frustrated total internal reflection (FTIR). Drags at speeds of 0.05, 0.1, 0.5, 1, and 10 mm s^{-1} were recorded at 250 fps. The adhesive's dynamic contact area was isolated in the image and digitized, with each pixel yielding a time-intensity waveform. We then performed a fast Fourier transform (FFT) analysis on the waveform, and averaged the FFT magnitude for each point to determine an average frequency response of the adhesive at a given speed.

Force and motion data were sampled at 1 kHz and recorded with software. A custom LabVIEW (National Instruments, Austin, TX) program controlled test parameters and data acquisition. Piezoelectric sensor drift was compensated for by fitting the zero-force variation before and after testing with a cubic spline in LabVIEW. Steady-state drag forces were calculated by averaging the forces between 25 and 75 per cent of the duration of the drag. We scaled the measured stiffness of setal arrays by area, A, and height (approx. 70 μm) to calculate the effective elastic modulus, $E_{\mathrm{eff}} = (70\,\mu\mathrm{m})k/A$, where k is the compressive stiffness of the setal array, as described in Autumn *et al.* (2006*c*). All results are mean ± standard error.

3. RESULTS

3.1. Rate dependence and wear resistance in gecko setae

Friction and adhesion forces were rate dependent (figure 2). Sliding arrays in their adhesive direction resulted in monotonically increasing magnitude of

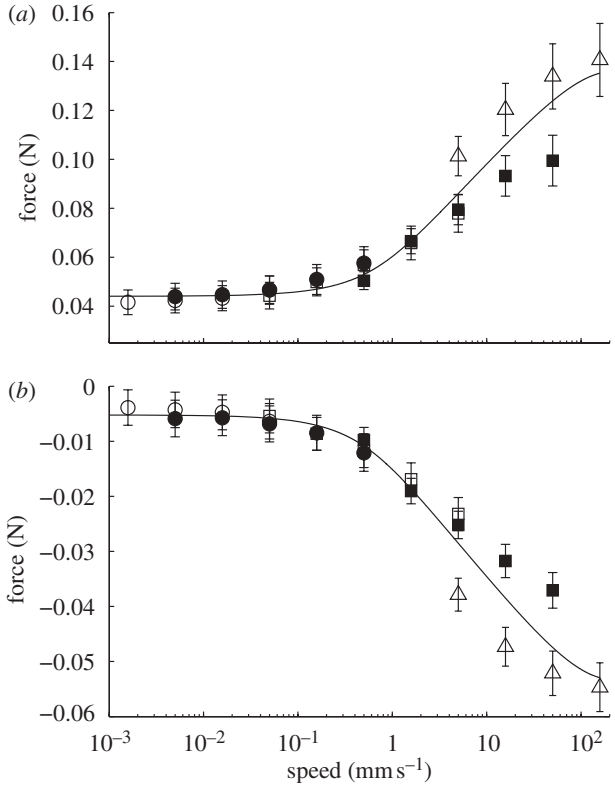

Figure 2. Steady-state contact forces increased in magnitude as a function of drag speed over drag distances of 10^{-3} mm (open circles), 10^{-2} mm (filled circles), 10^{-1} mm (open squares), 10^{0} mm (filled squares), and 10^{1} mm (open triangles). (*a*) Friction forces increased 3.3× over the velocity range. (*b*) Adhesion forces increased 10.3× over the test velocity range. Line fits are $F_{\mathrm{shear}} = (0.018\ \mathrm{N})(1 + v/(1.11 \times 10^3\ \mathrm{mm\ s^{-1}}))^{-1} \times \sinh^{-1}(v/(0.972\ \mathrm{mm\ s^{-1}})) + 0.044\ \mathrm{N}$ ($R^2 = 0.99$) and $F_{\mathrm{normal}} = -(0.009\ \mathrm{N})(1 + v/(1.11 \times 10^3\ \mathrm{mm\ s^{-1}}))^{-1} \sinh^{-1}(v/(0.751\ \mathrm{mm\ s^{-1}})) - 0.009\ \mathrm{N}$ ($R^2 = 0.99$).

friction–adhesion with speed. We measured an average 3.3× increase in friction and 10.3× increase in adhesion over the almost six orders of magnitude velocity test range (500 nm s^{-1}–158 mm s^{-1}). As setae transitioned from the static to the kinetic regime, frictional–adhesion forces remained consistent and did not decrease once the array began to slide, as would be predicted for typical dry, hard materials (figure 1).

Setal arrays were highly wear resistant. Over a battery of 30 000 load–drag–pulls of 10 mm displacement each, totaling 300 m of sliding, we measured a 25 per cent *increase* in adhesion and only a 5 per cent decrease in friction. Frictional–adhesion forces decreased initially, followed by a linear increase in contact forces (electronic supplementary material). We observed a 9 per cent decrease in the setal array effective elastic modulus over the 30 000 tests. During the velocity tests, we observed a larger 13 per cent decrease in average effective elastic modulus of 163 ± 19.2 kPa prior to testing, and 143 ± 14.8 kPa after testing (electronic supplementary material). The decrease in stiffness over repeated tests may have been due to an increase in alignment of the setae under repeated loading.

In total, we tested 25 setal array samples and rejected nine samples that completely or partially

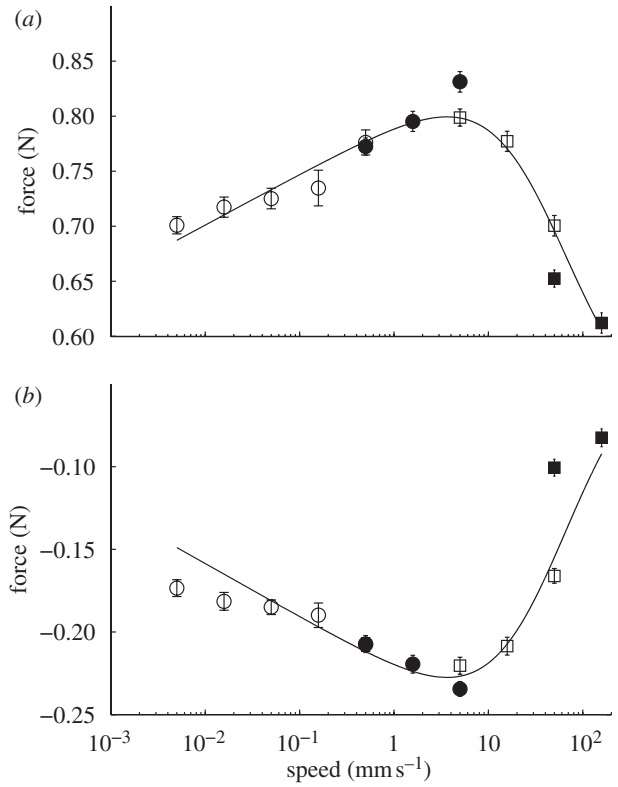

Figure 3. Steady-state contact forces of the GSA as a function of drag speed over drag distances of 10^{-1} mm (open circles), 10^{0} mm (filled circles), 10^{1} mm (open squares) and 3×10^{1} mm (filled squares). (*a*) Friction forces increased with speed until approximately 10 mm s^{-1} at which point friction decreased with speed. (*b*) Adhesion force followed the friction force. Line fits are $F_{\mathrm{shear}} = (0.020\ \mathrm{N})(1 + v/(52.4\ \mathrm{mm\ s^{-1}}))^{-1}\sinh^{-1}(v/(1.5\times 10^{-6}\ \mathrm{mm\ s^{-1}})) + 0.511\ \mathrm{N}$ ($R^2 = 0.96$) and $F_{\mathrm{normal}} = (-0.014\ \mathrm{N})(1 + v/(52.4\ \mathrm{mm\ s^{-1}}))^{-1}\sinh^{-1}(v/(1.5\times 10^{-6}\ \mathrm{mm\ s^{-1}})) - 0.025\ \mathrm{N}$ ($R^2 = 0.91$).

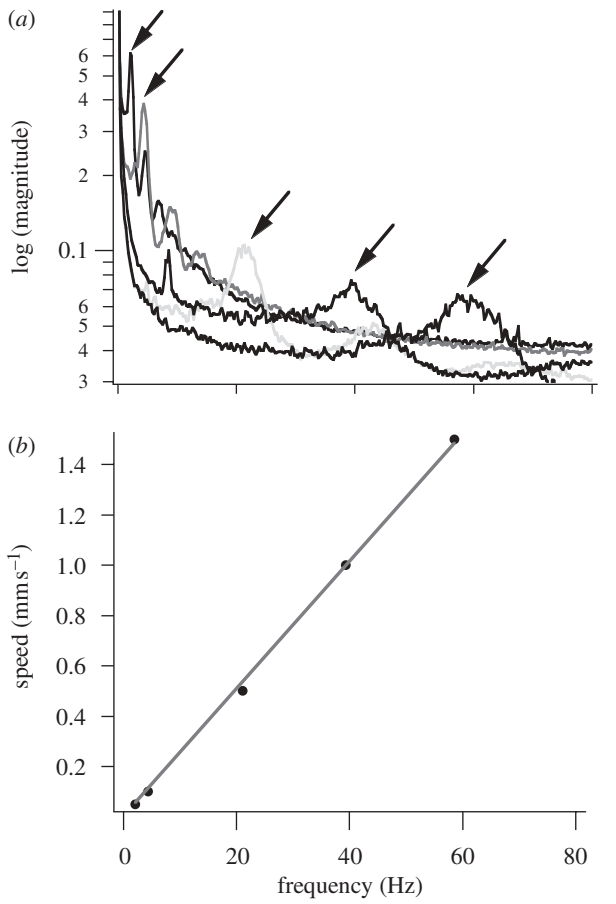

Figure 4. Stick–slip frequency analysis of the GSA. (*a*) The averaged FFT magnitude from high-speed video shows dominant stick–slip frequencies that increase in proportion to velocity. The 0.05, 0.10, 0.50, 1.00 and 1.50 mm s^{-1} FFT traces are highlighted with arrows from left to right in increasing order. (*b*) The dominant stick–slip frequencies (arrows) varied linearly with speed as $f = (25.3\ \mu\mathrm{m})v$. Using equation (4.4), the fit predicts a stick–slip displacement of $\lambda = 25.3\ \mu$m.

fractured from the SEM stub during testing. Five of the nine rejected samples tore from their mount at the highest shear speed of 158 mm s^{-1}, consistent with our observations that contact force was maximized at higher velocity. We rejected an additional two samples due to glue contamination from the mounting procedure, leaving 14 samples in our analysis.

3.2. Rate dependence and wear resistance in GSA

Friction and adhesion in the GSA were also velocity dependent. We observed logarithmically increasing frictional–adhesion forces with speed, which reached a maximum at 5 mm s^{-1} and steadily declined at higher speeds (figure 3). During shearing of the GSA, we observed uncorrelated stick–slip of the microscopic fibrils, while at the macroscopic scale, the adhesive slid smoothly. Durability measurements of the synthetic material exhibited only 7.2 per cent decrease in friction and 9.6 per cent decrease in adhesion over 30 000 tests totaling 300 m of sliding.

Using a high-speed video camera and FTIR, we observed stick–slip occurring in the frictionally adhering GSA. At drag speeds of 0.05, 0.50, 1 and 10 mm s^{-1}, we observed noticeable uncorrelated stick–slip events at the interface that could be observed by the naked eye. Performing an FFT analysis on the contact area determined by FTIR, imaged at 250 fps, we observed a dominant oscillation frequency at each speed corresponding to individual fibril stick–slip at the surface (figure 4). The stick–slip frequency varied linearly with speed ($f = (43.881\ \mathrm{mm^{-1}})v$) and the slope of this fit suggests a stick–slip distance of $\lambda = 25.3\ \mu$m, which we were able to confirm through microscopy.

4. DISCUSSION

When a gecko's toes slide, it does not detach from the surface, even if the surface is vertical or inverted (Huber *et al.* 2007; Jusufi *et al.* 2008), suggesting that gecko setae maintain adhesion and friction during sliding. Ordinarily, dry, hard materials slip more easily as they slide more rapidly, in part due to wear caused by rubbing (Bhushan 2002). Instead, we discovered that gecko setae became stickier as they slid more rapidly (figure 2), and resisted wear over a net displacement

of 300 m. We observed a threefold increase in friction and 10-fold increase in adhesion forces over shear velocities from 500 nm s^{-1} to 158 mm s^{-1}. The logarithmic increase in contact force in gecko setae is similar in form to that observed in polymer friction experiments (Vorvolakos & Chaudhury 2003; Vajpayee *et al.* 2009), raising the possibility that there is a common underlying mechanism despite the obvious differences in structure between gecko setal arrays and flat polymer surfaces.

Macroscale stick–slip is typically an unwanted behaviour that results in wear, chatter and unstable motion in sliding systems (Rabinowicz 1995; Bhushan 2002); however, nanoscale stick–slip dynamics are notably different (Gnecco *et al.* 2000; Richetti *et al.* 2001; Riedo *et al.* 2003; Tambe & Bhushan 2005), and it has been proposed that smooth macroscopic sliding may result from uncorrelated nanoscale stick–slip (Braun *et al.* 2005; Persson 1995). Nanoscale stick–slip models are ubiquitous in the mechanics of sliding solids (Rice & Ruina 1983; Baumberger *et al.* 1999; Gnecco *et al.* 2000; Richetti *et al.* 2001; Riedo *et al.* 2003; Tambe & Bhushan 2005; Bureau *et al.* 2006), elastomers (Chernyak & Leonov 1986; Schallamach 1963; Ghatak *et al.* 2000; Vorvolakos & Chaudhury 2003) and boundary lubricated systems (He & Robbins 2001; Richetti *et al.* 2001; Tao & Bhushan 2007). We propose that wear resistance, and stable frictional adhesion forces during sliding, may emerge from the stochastic stick–slip of a population of individual fibrils with high resonant frequencies.

4.1. A stick–slip model of kinetic friction and adhesion

In a fibrillar adhesive, contact stress should be evenly distributed among the fibrils (Hui *et al.* 2004). Therefore, considering the high modulus of keratin (Peattie *et al.* 2007), it is reasonable to assume that during sliding, setal shafts remain in tension and are effectively rigid (Gravish *et al.* 2007), while the spatular shafts undergo uncorrelated stick–slip. To model stick–slip of a spatular shaft (fibril), we assume that during sliding, fibrils cycle through a stick–slip process governed by two characteristic times: t_{stick}, the average lifetime of a fibril–substrate bond, and τ_0, the characteristic time for a fibril to reattach to the substrate after bond rupture. Assuming fibrils act as vertical or curved cantilever beams (Jagota & Bennison 2002; Sitti & Fearing 2003; Hui *et al.* 2004; Autumn *et al.* 2006*c*; Gravish *et al.* 2007; Chen *et al.* 2008; figure 5), we estimate the characteristic reattachment time to be given by $\tau_0 = 1/f$, where f is the fibre's resonant frequency. Assuming a purely elastic system, a cylindrical fibre of material density ρ, radius R, area $A = \pi R^2$, length l, Young's modulus E and bending inertia $I = \pi R^4/4$,

$$\tau_0 = \frac{1}{f} = 2\pi\sqrt{\frac{\rho A l^4}{8EI}}. \tag{4.1}$$

The slip time (equal to τ_0) is independent of sliding velocity (v), whereas the stick time (t_{stick}) is a function of v and a characteristic yield displacement (λ) at which the adhesive bond is broken. Thus, the average lifetime of a fibril bond is given by

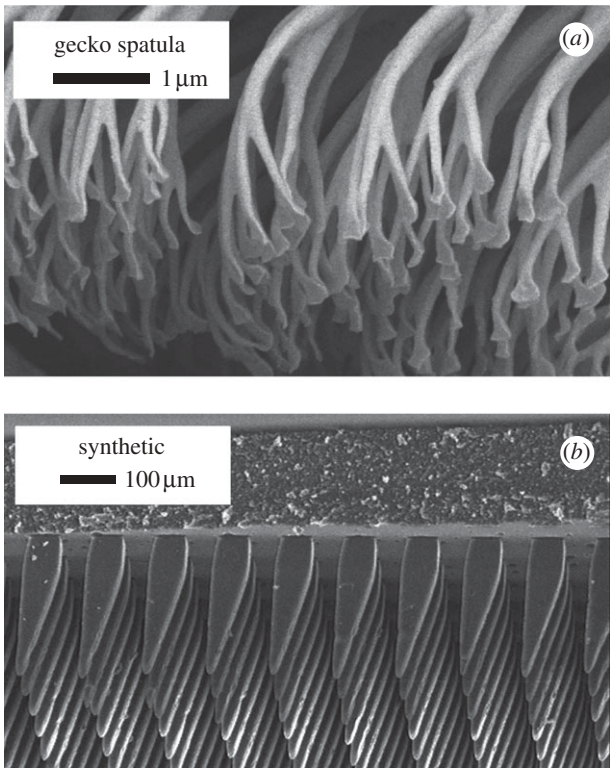

Figure 5. Fibrillar geometry of (*a*) natural gecko setae and (*b*) GSA.

$$t_{\mathrm{stick}} = \frac{\lambda}{v}. \tag{4.2}$$

Our assumption here is that the fibril–surface contact will break when the macroscopic array has moved by a distance λ. The microscopic details are unknown at this point but could involve a combination of stretching of the spatula (Yamaguchi *et al.* 2009) and rate-dependent plastic yielding of the actual contact as suggested in the state and rate model (Baumberger *et al.* 1999).

To analyse the stick–slip response of fibrillar adhesives, we employ a dimensionless Deborah number (Reiner 1964; Huilgol 1975; Israelachvili & Berman 1995), which is ordinarily defined in rheology as the ratio of the characteristic relaxation time of the system to the observation time. For stick–slip systems, however, we can define the Deborah number as

$$\mathrm{De}(v) = v/V^*, \tag{4.3}$$

the ratio of the sliding velocity (v) to the critical relaxation velocity V^*, the ratio of the slip length λ to the characteristic time τ_0 (Richetti *et al.* 2001; Filippov *et al.* 2004):

$$V^* = \frac{\lambda}{\tau_0}. \tag{4.4}$$

The critical relaxation velocity defines an inflection point in the adhesive's sliding behaviour; above V^*, individual fibrils spend more time reattaching to the substrate than they do sticking to it. Consider N_0

fibrils undergoing stick–slip: the number of fibrils attached to the substrate simultaneously is given by (Schallamach 1963)

$$N(v) = N_0 \frac{1}{1 + \mathrm{De}(v)}. \tag{4.5}$$

When the system is driven at a velocity lower than V^*, then $\mathrm{De} < 1$, and fibrils are predominantly stuck to the substrate with reattachment occurring rapidly relative to the speed of the substrate. At low $v \ll V^*$, $N(v)$ is near N_0. When the system is driven at a velocity faster than V^*, then $\mathrm{De} > 1$, and the reattachment time becomes slow compared with the motion of the substrate. At $v \gg V^*$, the response of the system becomes consistent with the decline in force with velocity expected in friction between solids in contact (Rice & Ruina 1983; Baumberger *et al.* 1999). In this case, force declines with velocity because fewer fibrils can attach simultaneously as velocity increases.

We can now estimate the model predictions for gecko spatulae. In tokay geckos, flat spatula pads ($200 \times 300 \times 5$ nm pads) are attached to approximately 800 nm long × 50 nm diameter shafts (Ruibal & Ernst 1965; Russell 1975; Williams & Peterson 1982; Tian *et al.* 2006). Keratin modulus is $E = 1.5$ GPa (Peattie *et al.* 2007) and we assume a density of $\rho = 1000$ kg m^{-3}. Thus, for fibrils of $l = 800$ nm, $R = 25$ nm, bending inertia is $I = 3.07 \times 10^{-31}$ m^4, and equation (4.1) yields a characteristic time of $\tau_0 = 0.09$ μs for relaxation of the fibril during slip and a natural frequency of 10.8 MHz. Adhering spatulae are between 100 and 1000 nm apart and single spatula measurements typically observe vertical detachment within 100–1000 nm displacement (Huber *et al.* 2005*a*; Sun *et al.* 2005). Therefore, we use $\lambda = 100$ nm as a conservative lower bound of the slip length of the spatula, yielding a predicted critical velocity $V^* = 100$ nm/0.09 μs $= 1.08$ m s^{-1} (equation (4.4)). This suggests that $\mathrm{De} \ll 1$ over our entire experimental velocity range (500 nm s^{-1}–158 mm s^{-1}; equation (4.3)) because V^* is at least 1 m s^{-1} in gecko setae.

4.2. Rate dependence of detachment force

The last, but important, point that remains to be discussed is the detachment condition for the spatulae. If the detachment force was independent of t_{stick}, then for $\mathrm{De} < 1$, the time-averaged force could only be constant with increasing velocity, which is inconsistent with the experimental data. This suggests that the force to detach a spatula $f(v)$ is not independent of t_{stick}, but increases as t_{stick} decreases, i.e. as the strain rate of the spatulae increases, as discussed by Yamaguchi *et al.* (2009).

The velocity dependence of the gecko adhesive and GSA was logarithmic above a threshold speed (figures 2 and 3). Logarithmic force–velocity models are abundant in the mechanics of atomic stick–slip (Bennewitz *et al.* 1999; Gnecco *et al.* 2000; Richetti *et al.* 2001; Riedo *et al.* 2003; Tambe & Bhushan 2005; Tao & Bhushan 2007), yielding in polymers (Mulliken 2004; Ward & Sweeney 2004; Bureau *et al.* 2006; Mulliken & Boyce 2006), elastomer friction (Schallamach 1963; Vorvolakos & Chaudhury 2003; Vajpayee *et al.* 2009) and boundary lubricated surfaces (He & Robbins 2001; Richetti *et al.* 2001; Tao & Bhushan 2007). To model our data, we apply a velocity-dependent function that is constant at low velocity, and logarithmic at higher velocity

$$F(v) \approx \sigma_0 \sinh^{-1}\left(\frac{v}{v_0}\right), \tag{4.6}$$

where v is the macroscopic relative motion between the setal array and the substrate and v_0 is an adjustable parameter setting the velocity where F is proportional to σ_0.

We can now model the rate dependence of the total force of a fibrillar array (F_{array}) by combining equation (4.5) (the rate dependence of number of contacts) and equation (4.6) (the rate dependence of the force of each contact):

$$\begin{aligned} F_{\mathrm{array}}(v) &= N(v) \cdot F(v) \\ &\approx N_0 \frac{1}{1 + \mathrm{De}(v)} \sigma_0 \sinh^{-1}\left(\frac{v}{v_0}\right) + F_0, \end{aligned} \tag{4.7}$$

$$F_{\mathrm{array}}(v) \approx N_0 \left(1 + \frac{v}{\lambda f}\right)^{-1} \sigma_0 \sinh^{-1}\left(\frac{v}{v_0}\right) + F_0. \tag{4.8}$$

It is worthwhile to note that rate-dependent stick–slip models of polymer yielding (Krausz & Eyring 1975; Ward & Sweeney 2004), elastomer friction (Schallamach 1963; Vorvolakos & Chaudhury 2003), boundary lubricated friction (He & Robbins 2001; Richetti *et al.* 2001; Tao & Bhushan 2007), atomic stick–slip (Bennewitz *et al.* 1999; Gnecco *et al.* 2001; Riedo *et al.* 2003; Tambe & Bhushan 2005) and even earthquakes (Huisman & Fasolino 2005) all suggest that smooth macroscopic kinetic friction is the result of uncorrelated stick–slip of all the discrete microscale contact elements sliding along the surface, precisely what we observed in the GSA and what we predicted for gecko setae.

It may be the case that gecko spatulae are subject to rate-dependent yielding during stick–slip, as in unlubricated friction of polymer glasses (Creton *et al.* 1999; Bureau *et al.* 2006). As discussed earlier, spatulae are not elastomers, but rather are made of β-keratin, a stiff material (Rizzo *et al.* 2006; Peattie *et al.* 2007) analogous to a polymer glass. Sliding of polymer glasses on a smooth surface occurs as microscopic contact points move by shearing of highly localized nanoscopic layers that are deformed beyond the yield stress of the polymer. Fracture of spatular contacts in mixed mode (shear and tension) may then involve local plasticity at the interface between the spatula and the surface. An order of magnitude estimate for the plausibility of this mechanism comes from measurements of individual setae. A single seta can sustain 200 μN in shear (Autumn *et al.* 2000). Assuming approximately 500 spatulae per seta, the shear force is 0.4 μN per spatula, which is supported by an area of roughly 0.01 μm^2. The average shear stress to be transferred to the surface by each spatula is then of the order 40 μN μm^{-2} or 40 MPa, of the order of magnitude of the yield stress of a molecular solid such as β-keratin. Further microscopic investigations will elucidate this issue.

4.3. Rate dependence and wear resistance in GSA

Shearing the GSA resulted in smooth friction and adhesion forces during macroscopic sliding while stick–slip events at the fibrillar level were visible at the microscale (see video in the electronic supplementary material). While some GSA fibrils slid steadily, stick–slip was the dominant mechanism, accounting for the remarkable durability of the GSA, which maintained over 90 per cent of its adhesion over a total sliding distance of 300 m. The stick–slip model predicts that the frequency of stick events (f) should vary linearly with the drag velocity as $v = \lambda f$. As predicted (equation (4.2)), stick–slip frequency varied linearly with velocity (figure 4; $v = (25.3\ \mu\text{m})f$; $R^2 = 0.99$) and from the slope of this fit and equation (4.2), we estimate that the 155 μm tall GSA structures have a characteristic stick–slip distance of $\lambda = 25.3\ \mu\text{m}$, which was similar to the displacements observed visually (23 μm). This confirms that smooth, macroscopic friction–adhesion can result from uncorrelated stick–slip events at the fibrillar level.

It is clear that significant differences exist between the sliding motion of natural gecko setae and that of the GSA (compare the electronic supplementary material of this study with the electronic supplementary material of Gravish *et al.* (2007; http://rsif.royalsocietypublishing.org/content/5/20/339/suppl/DC1)). This may be due in part to the difference in dissipative mechanisms resisting detachment (viscoelastic for the Sylgard elastomer and plastic for the keratin), so we must be cautious about the direct applicability of the GSA results to the gecko system.

We determined V^* for the GSA experimentally (figure 3) and then compared it with a prediction based on the resonant frequency of a PDMS cantilever. To predict V^* in the GSA, we estimated the natural frequency of a tapered beam (Volterra & Zachmanoglou 1965) as

$$f = 2.675 \frac{H}{2\pi l^2} \sqrt{\frac{E}{3\rho}}. \tag{4.9}$$

For our structures (see §2), $E = 1.75$ MPa, $\rho = 1370\ \text{kg m}^{-3}$, $H = 45\ \mu\text{m}$ and $l = 155\ \mu\text{m}$, yielding a natural frequency of 15.8 kHz and a characteristic time $\tau_0 = 63\ \mu\text{s}$. We observed a slip distance of $\lambda = 23\ \mu\text{m}$. Therefore, the predicted critical velocity (equation (4.4)) is $V^* = 364\ \text{mm s}^{-1}$, roughly two orders of magnitude larger than the observed velocity at which forces were maximal (figure 3). The prediction (equation (4.9)) does not account for the elastomeric backing layer that the GSA array is mounted upon, nor any damping in the material. Moreover, estimating f from equation (4.9) assumes that fibres return to their unloaded state without resistance. In contrast, we observed that following detachment, fibres maintained frictional contact with the surface while relaxing to a freestanding position (electronic supplementary material). Our calculation (equation 4.9) represents an upper bound to the GSA's critical velocity and the difference in our measured V^* suggests that friction and surface dynamics play at least as important a role as the free resonant response.

4.4. Why geckos do not fall when they slip

Selection for dynamic locomotion in unpredictable environments may have driven the evolution of adhesive nanostructures in geckos. Slip resistance in biological attachment mechanisms has evolved through the use of fluids (Denny 1980; Federle *et al.* 2006) or compliant materials (Gorb 1998; Federle *et al.* 2004; Santos *et al.* 2005). Instead, geckos evolved branched setal arrays made of a high modulus material (1.5 GPa; Peattie *et al.* 2007) with millions of redundant high-aspect ratio contact points, each with a very high resonant frequency (10 MHz), resulting in a novel dry adhesive that responds to sliding by becoming stickier. This is why geckos do not fall when their toes slide. If the rate of sliding is lower than the critical velocity V^* (approx. $1\ \text{m s}^{-1}$), then $\text{De} < 1$ and the majority of spatulae undergoing stick–slip will be sticking to the substrate simultaneously. This design also promotes wear resistance since sliding at the macroscale can occur while individual contacts remain static. Dynamic friction alone could be the functional role for non-adhesive setae in phylogenetically basal geckos such as *Aeluroscalabotes felinus* (Peattie & Full 2007), which represent a puzzling intermediate evolutionary step between the nano-spiny epidermis of gecko ancestors, and highly adhesive branched setae of derived geckos.

4.5. Design of failure-resistant GSAs

Our results and model suggest design principles for the development of GSAs. Approaching the performance of the gecko will require a very fine hierarchical structure of fibrils made of a hard material, which is difficult to manufacture. Yet, recent results showing strong static attachment and shear adhesion (Lee *et al.* 2008; Qu *et al.* 2008; Schubert *et al.* 2008; Vajpayee *et al.* 2009) are promising.

The principle of uncorrelated stick–slip motion can be applied to softer and larger structures, as demonstrated in our GSA. As the fibril size increases, the elastic energy of deformation of the fibril will become more important relative to adhesive forces. Therefore, it becomes necessary to use a softer material such as a rubber for the fibrils. A viscoelastic rubber would seem a good choice for maximizing pull-off force because of the high dissipation at each crack tip, as contacts start to peel. However, maximization of pull-off is not ideal for dynamic applications such as climbing robots (Autumn *et al.* 2005; Kim *et al.* 2007), where for safety, it is desirable to maintain, or even increase, the aggregate shear and adhesive forces when sliding occurs. The good sliding performance of the GSA (figure 3) was a consequence of using a PDMS elastomer with relatively low damping. In contrast, GSAs fabricated from a more dissipative urethane elastomer had high adhesion statically, but performance declined rapidly at the onset of sliding (Santos *et al.* 2007; Santos 2009).

5. CONCLUSIONS

The gecko adhesive is a rich and complex tribological system. Recent theoretical attempts to reconcile molecular dynamics and empirical tribology results have proposed that macroscopically smooth sliding can be the result of a population of stick–slip events at the atomic scale (Braun *et al.* 2005; Huisman & Fasolino 2005). Our observations support this model and suggest that the dynamics of gecko setae and GSAs may be of interest to scientists studying macro- to nanoscale phenomena as diverse as earthquakes (Rice 1980; Carlson *et al.* 1994; Heslot *et al.* 1994) and atomic friction (Bennewitz *et al.* 1999; Gnecco *et al.* 2001; Riedo *et al.* 2003; Tambe & Bhushan 2005).

We thank Jacob Israelachvili, Anne Peattie and three anonymous reviewers for helpful comments. Work performed at the Stanford Nanofabrication Facility of NNIN was supported by the National Science Foundation under grant ECS-9731293. This work was also supported in part by DARPA-Zman, NSF Center of Integrated Nanomechanical Systems and CIS New Users Grant Program. Work performed at Lewis & Clark College was supported by NSF-NIRT 0304730 and DCI/NGIA HM1582-05-2022 grants to K.A.

REFERENCES

Alibardi, L. 2003 Ultrastructural autoradiographic and immunocytochemical analysis of setae formation and keratinization in the digital pads of the gecko *Hemidactylus turcicus* (Gekkonidae, Reptilia). *Tissue Cell* **35**, 288–296. (doi:10.1016/S0040-8166(03)00050-8)

Aristotle 350 BCE 1918 *Historia animalium* (transl. by D. W. Thompson). Oxford, UK: The Clarendon Press.

Arzt, E., Gorb, S. & Spolenak, R. 2003 From micro to nano contacts in biological attachment devices. *Proc. Natl Acad. Sci USA* **100**, 10 603–10 606. (doi:10.1073/pnas.1534701100)

Autumn, K. 2006 Properties, principles, and parameters of the gecko adhesive system. In *Biological adhesives* (eds A. Smith & J. Callow), pp. 225–255. Berlin, Germany: Springer Verlag.

Autumn, K. & Hansen, W. 2006 Ultrahydrophobicity indicates a nonadhesive default state in gecko setae. *J. Comp. Physiol. A* **192**, 1205–1212. (doi:10.1007/s00359-006-0149-y)

Autumn, K., Liang, Y. A., Hsieh, S. T., Zesch, W., Chan, W.-P., Kenny, W. T., Fearing, R. & Full, R. J. 2000 Adhesive force of a single gecko foot-hair. *Nature* **405**, 681–685. (doi:10.1038/35015073)

Autumn, K. *et al.* 2002 Evidence for van der Waals adhesion in gecko setae. *Proc. Natl Acad. Sci. USA* **99**, 12 252–12 256. (doi:10.1073/pnas.192252799)

Autumn, K. *et al.* 2005. Robotics in scansorial environments. *Proc. SPIE* **5804**, 291–302. (doi:10.1117/12.606157)

Autumn, K., Dittmore, A., Santos, D., Spenko, M. & Cutkosky, M. 2006*a* Frictional adhesion: a new angle on gecko attachment. *J. Exp. Biol.* **209**, 3569–3579. (doi:10.1242/jeb.02486)

Autumn, K., Hsieh, S. T., Dudek, D. M., Chen, J., Chitaphan, C. & Full, R. J. 2006*b* Dynamics of geckos running vertically. *J. Exp. Biol.* **209**, 260–272. (doi:10.1242/jeb.01980)

Autumn, K., Majidi, C., Groff, R., Dittmore, A. & Fearing, R. 2006*c* Effective elastic modulus of isolated gecko setal arrays. *J. Exp. Biol.* **209**, 3558–3568. (doi:10.1242/jeb.02469)

Autumn, K., Gravish, N., Wilkinson, M., Santos, D., Spenko, M. & Cutkosky, M. 2007. Frictional adhesion of natural and synthetic gecko setal arrays. In *Proc. 30th Annu. Meeting of the Adhesion Society*, pp. 58–60.

Baumberger, T., Berthoud, P. & Caroli, C. 1999 Physical analysis of the state- and rate-dependent friction law. II. Dynamic friction. *Phys. Rev. B* **60**, 3928–3939. (doi:10.1103/PhysRevB.60.3928)

Bennewitz, R., Gyalog, T., Guggisberg, M., Bammerlin, M., Meyer, E. & Guntherodt, H. J. 1999 Atomic-scale stick-slip processes on Cu(111). *Phys. Rev. B* **60**, R11 301–R11 304. (doi:10.1103/PhysRevB.60.R11301)

Bhushan, B. 2002 *Introduction to tribology*. New York, NY: John Wiley & Sons.

Bhushan, B., Galasso, B., Bignardi, C., Nguyen, C., Dai, L. & Qu, L. 2008 Adhesion, friction and wear on the nanoscale of MWNT tips and SWNT and MWNT arrays. *Nanotechnology* **19**, 125 702. (doi:10.1088/0957-4484/19/12/125702)

Braun, O. M., Peyrard, M., Bortolani, V., Franchini, A. & Vanossi, A. 2005 Transition from smooth sliding to stick-slip motion in a single frictional contact. *Phys. Rev. E* **72**, 056116. (doi:10.1103/PhysRevE.72.056116)

Bullock, J. M. R., Drechsler, P. & Federle, W. 2008 Comparison of smooth and hairy attachment pads in insects: friction, adhesion and mechanisms for direction-dependence. *J. Exp. Biol.* **211**, 3333–3343. (doi:10.1242/jeb.020941)

Bureau, L., Caroli, C. & Baumberger, T. 2006 Frictional dissipation and interfacial glass transition of polymeric solids. *Phys. Rev. Lett.* **97**, 225 501. (doi:10.1103/PhysRevLett.97.225501)

Carlson, J. M., Langer, J. S. & Shaw, B. E. 1994 Dynamics of earthquake faults. *Rev. Mod. Phys.* **66**, 657–670. (doi:10.1103/RevModPhys.66.657)

Chen, B., Wu, P. D. & Gao, H. 2008 Hierarchical modelling of attachment and detachment mechanisms of gecko toe adhesion. *Proc. R. Soc. A* **464**, 1639–1652. (doi:10.1098/rspa.2007.0350)

Chen, B., Wu, P. D. & Gao, H. 2009 Pre-tension generates strongly reversible adhesion of a spatula pad on substrate. *J. R. Soc. Interface* **6**, 529–537. (doi:10.1098/rsif.2008.0322)

Chernyak, Y. B. & Leonov, A. I. 1986 On the theory of the adhesive friction of elastomers. *Wear* **108**, 105–138. (doi:10.1016/0043-1648(86)90092-X)

Creton, C. 2003 Pressure-sensitive adhesives: an introductory course. *MRS Bull.* **28**, 434–439.

Creton, C., Halary, J. L. & Monnerie, L. 1999 Plasticity of polystyrene-poly(2,6,dimethyl,1,4,phenylene oxide) blends. *Polymer* **40**, 199–206. (doi:10.1016/S0032-3861(98)00206-7)

Denny, M. 1980 The role of gastropod pedal mucus in locomotion. *Nature* **285**, 160–161. (doi:10.1038/285160a0)

Eimuller, T., Guttmann, P. & Gorb, S. N. 2008 Terminal contact elements of insect attachment devices studied by transmission X-ray microscopy. *J. Exp. Biol.* **211**, 1958–1963. (doi:10.1242/jeb.014308)

Federle, W., Baumgartner, W. & Holldobler, B. 2004 Biomechanics of ant adhesive pads: frictional forces are rate- and temperature-dependent. *J. Exp. Biol.* **207**, 67–74. (doi:10.1242/jeb.00716)

Federle, W., Barnes, W. J. P., Baumgartner, W., Drechsler, P. & Smith, J. M. 2006 Wet but not slippery: boundary friction in tree frog adhesive toe pads. *J. R. Soc. Interface* **3**, 689–697. (doi:10.1098/rsif.2006.0135)

Filippov, A. E., Klafter, J. & Urbakh, M. 2004 Friction through dynamical formation and rupture of molecular bonds. *Phys. Rev. Lett.* **92**, 135 503. (doi:10.1103/PhysRevLett.92.135503)

Ghatak, A., Vorvolakos, K., She, H. Q., Malotky, D. L. & Chaudhury, M. K. 2000 Interfacial rate processes in

adhesion and friction. *J. Phys. Chem. B* **104**, 4018–4030. (doi:10.1021/jp9942973)

Gnecco, E., Bennewitz, R., Gyalog, T., Loppacher, C., Bammerlin, M., Meyer, E. & Guntherodt, H. J. 2000 Velocity dependence of atomic friction. *Phys. Rev. Lett.* **84**, 1172–1175. (doi:10.1103/PhysRevLett.84.1172)

Gnecco, E., Bennewitz, R., Gyalog, T. & Meyer, E. 2001 Friction experiments on the nanometre scale. *J. Phys. Condens. Matter* **13**, R619–R642. (doi:10.1088/0953-8984/13/31/202)

Gorb, S. N. 1998 The design of the fly adhesive pad: distal tenent setae are adapted to the delivery of an adhesive secretion. *Proc. R. Soc. Lond. B* **265**, 747–752. (doi:10.1098/rspb.1998.0356)

Gravish, N., Wilkinson, M. & Autumn, K. 2007 Frictional and elastic energy in gecko adhesive detachment. *J. R. Soc. Interface* **5**, 339–348. (doi:10.1098/rsif.2007.1077)

Hansen, W. & Autumn, K. 2005 Evidence for self-cleaning in gecko setae. *Proc. Natl Acad. Sci. USA* **102**, 385–389. (doi:10.1073/pnas.0408304102)

He, G. & Robbins, M. O. 2001 Simulations of the kinetic friction due to adsorbed surface layers. *Tribology Lett.* **10**, 7–14. (doi:10.1023/A:1009030413641)

Heslot, F., Baumberger, T., Perrin, B., Caroli, B. & Caroli, C. 1994 Creep, stick-slip, and dry-friction dynamics—experiments and a heuristic model. *Phys. Rev. E* **49**, 4973–4988. (doi:10.1103/PhysRevE.49.4973)

Huber, G., Gorb, S., Spolenak, R. & Arzt, E. 2005*a* Resolving the nanoscale adhesion of individual gecko spatulae by atomic force microscopy. *Biol. Lett.* **1**, 2–4. (doi:10.1098/rsbl.2004.0254)

Huber, G., Mantz, H., Spolenak, R., Mecke, K., Jacobs, K., Gorb, S. & Arzt, E. 2005*b* Evidence for capillarity contributions to gecko adhesion from single spatula nanomechanical measurements. *Proc. Natl Acad. Sci. USA* **102**, 16 293–16 296. (doi:10.1073/pnas.0506328102)

Huber, G., Gorb, S., Hosoda, N., Spolenak, R. & Arzt, E. 2007 Influence of surface roughness on gecko adhesion. *Acta Biomater.* **3**, 607–610. (doi:10.1016/j.actbio.2007.01.007)

Hui, C. Y., Glassmaker, N. J., Tang, T. & Jagota, A. 2004 Design of biomimetic fibrillar interfaces: 2. Mechanics of enhanced adhesion. *J. R. Soc. Interface* **1**, 35–48. (doi:10.1098/rsif.2004.0005)

Hui, C. Y., Shen, L., Jagota, A. & Autumn, K. 2006 Mechanics of anti-fouling or self-cleaning in gecko setae. In *Proc. 29th Annu. Meeting of the Adhesion Society.*

Huilgol, R. R. 1975 On the concept of the Deborah number. *Trans. Soc. Rheology* **19**, 297–306. (doi:10.1122/1.549372)

Huisman, B. A. H. & Fasolino, A. 2005 Transition to strictly solitary motion in the Burridge–Knopoff model of multicontact friction. *Phys. Rev. E* **72**, 016 107. (doi:10.1103/PhysRevE.72.016107)

Israelachvili, J. 1992 *Intermolecular and surface forces.* New York, NY: Academic Press.

Israelachvili, J. N. 2005 Engineering—skimming the surface. *Nature* **435**, 893–895. (doi:10.1038/435893a)

Israelachvili, J. & Berman, A. 1995 Irreversibility, energy-dissipation, and time effects in intermolecular and surface interactions. *Isr. J. Chem.* **35**, 85–91.

Jagota, A. & Bennison, S. 2002 Mechanics of adhesion through a fibrillar microstructure. *Int. Comp. Biol.* **42**, 1140–1145. (doi:10.1093/icb/42.6.1140)

Jusufi, A., Goldman, D., Revzen, S. & Full, R. 2008 Active tails enhance arboreal acrobatics in geckos. *Proc. Natl Acad. Sci. USA* **105**, 4215–4219. (doi:10.1073/pnas.0711944105)

Kim, S., Spenko, M., Trujillo, S., Heyneman, B., Mattoli, V. & Cutkosky, M. R. 2007 Whole body adhesion: hierarchical, directional and distributed control of adhesive forces for a climbing robot. In *IEEE Int. Conf. on Robotics and Automation, Rome, Italy*, pp. 1268–1273.

Krausz, A. S. & Eyring, H. 1975 *Deformation kinetics.* New York, NY: John Wiley & Sons.

Krim, J. 1996 Friction at the atomic scale. *Sci. Am.* **275**, 74–80.

Lamb, T. & Bauer, A. M. 2006. Footprints in the sand: independent reduction of subdigital lamellae in the Namib–Kalahari burrowing geckos. *Proc. R. Soc. B* **273**, 855–864. (doi:10.1098/rspb.2005.3390)

Lee, J. & Fearing, R. S. 2008 Contact self-cleaning of synthetic gecko adhesive from polymer microfibers. *Langmuir* **24**, 10 587–10 591. (doi:10.1021/la8021485)

Lee, J., Majidi, C., Schubert, B. & Fearing, R. S. 2008 Sliding induced adhesion of stiff polymer microfiber arrays: 1. Macroscale bahaviour. *J. R. Soc. Interface* **5**, 835–844. (doi:10.1098/rsif.2007.1308)

Luan, B. Q. & Robbins, M. O. 2005 The breakdown of continuum models for mechanical contacts. *Nature* **435**, 929–932. (doi:10.1038/nature03700)

Maderson, P. F. A. 1964 Keratinized epidermal derivatives as an aid to climbing in gekkonid lizards. *Nature* **203**, 780–781. (doi:10.1038/203780a0)

Mulliken, A. 2004 Low to high strain rate deformation of amorphous polymers: experiments and modeling. MS thesis, Department of Mechanical Engineering, MIT.

Mulliken, A. & Boyce, M. 2006 Mechanics of the rate-dependent elastic–plastic deformation of glassy polymers from low to high strain rates. *Int. J. Solids Struct.* **43**, 1331–1356. (doi:10.1016/j.ijsolstr.2005.04.016)

Parness, A., Soto, D., Esparza, N., Gravish, N., Wilkinson, M., Autumn, K. & Cutkosky, M. In press. A microfabricated wedge-shaped adhesive array displaying gecko-like dynamic adhesion, directionality and long lifetime. *J. R. Soc. Interface* **6**, 1223–1232. (doi:10.1098/rsif.2009.0048)

Peattie, A. M. & Full, R. J. 2007. Phylogenetic analysis of the scaling of wet and dry biological fibrillar adhesives. *Proc. Natl Acad. Sci. USA* **104**, 18 595–18 600. (doi:10.1073/pnas.0707591104)

Peattie, A. M., Majidi, C., Corder, A. & Full, R. J. 2007 Ancestrally high elastic modulus of gecko setal β-keratin. *J. R. Soc. Interface* **4**, 1071–1076. (doi:10.1098/rsif.2007.0226)

Persson, B. N. J. 1995 Theory of friction—stress domains, relaxation, and creep. *Phys. Rev. B* **51**, 13 568–13 585. (doi:10.1103/PhysRevB.51.13568)

Persson, B. N. J. 2003 On the mechanism of adhesion in biological systems. *J. Chem. Phys.* **118**, 7614–7621. (doi:10.1063/1.1562192)

Pianka, E. R. & Sweet, S. S. 2005 Integrative biology of sticky feet in geckos. *BioEssays* **27**, 647–652. (doi:10.1002/bies.20237)

Pocius, A. V. 2002 *Adhesion and adhesives technology: an introduction*, 2nd edn. Munich, Germany: Hanser Verlag.

Porto, M., Zaloj, V., Urbakh, M. & Klafter, J. 2000 Macroscopic versus microscopic description of friction. *Tribology Lett.* **9**, 45–54. (doi:10.1023/A:1018800309732)

Qu, L. T., Dai, L. M., Stone, M., Xia, Z. H. & Wang, Z. L. 2008 Carbon nanotube arrays with strong shear binding-on and easy normal lifting-off. *Science* **322**, 238–242. (doi:10.1126/science.1159503)

Rabinowicz, E. 1995 *Friction and wear of materials.* New York, NY: Wiley-Interscience.

Reiner, M. 1964 The Deborah number. *Phys. Today* **17**, 62. (doi:10.1063/1.3051374)

Rice, J. R. 1980 The mechanics of earthquake rupture. In *Physics of the earth's interior* (eds A. M. Dziewonski &

E. Boschi), pp. 555–649. Amsterdam, The Netherlands: Italian Physical Society and North-Holland.

Rice, J. R. & Ruina, A. L. 1983 Stability of steady frictional slipping. *J. Appl. Mech. Trans. ASME* **50**, 343–349.

Richetti, P., Drummond, C., Israelachvili, J., In, M. & Zana, R. 2001 Inverted stick-slip friction. *Europhys. Lett.* **55**, 653–659. (doi:10.1209/epl/i2001-00109-0)

Riedo, E., Gnecco, E., Bennewitz, R., Meyer, E. & Brune, H. 2003 Interaction potential and hopping dynamics governing sliding friction. *Phys. Rev. Lett.* **91**, 084 502. (doi:10.1103/PhysRevLett.91.084502)

Ringlein, J. & Robbins, M. O. 2004 Understanding and illustrating the atomic origins of friction. *Am. J. Phys.* **72**, 884–891. (doi:10.1119/1.1715107)

Rizzo, N., Gardner, K., Walls, D., Keiper-Hrynko, N., Ganzke, T. & Hallahan, D. 2006 Characterization of the structure and composition of gecko adhesive setae. *J. R. Soc. Interface* **3**, 441–451. (doi:10.1098/rsif.2005.0097)

Robbins, M. O. & Smith, E. D. 1996 Connecting molecular-scale and macroscopic tribology. *Langmuir* **12**, 4543–4547. (doi:10.1021/la9505576)

Ruibal, R. & Ernst, V. 1965 The structure of the digital setae of lizards. *J. Morphol.* **117**, 271–294. (doi:10.1002/jmor.1051170302)

Russell, A. P. 1975 A contribution to the functional morphology of the foot of the tokay, *Gekko gecko* (Reptilia, Gekkonidae). *J. Zool. Lond.* **176**, 437–476.

Santos, D. O. 2009 Contact modeling and directional adhesion for climbing robots. PhD thesis, Stanford University.

Santos, R., Gorb, S., Jamar, V. & Flammang, P. 2005 Adhesion of echinoderm tube feet to rough surfaces. *J. Exp. Biol.* **208**, 2555–2567. (doi:10.1242/jeb.01683)

Santos, D., Spenko, M., Parness, A., Kim, S. & Cutkosky, M. 2007 Directional adhesion for climbing: theoretical and practical considerations. *J. Adh. Sci. Technol.* **21**, 1317–1341. (doi:10.1163/156856107782328399)

Schallamach, A. 1963 A theory of dynamic rubber friction. *Wear* **6**, 375–382. (doi:10.1016/0043-1648(63)90206-0)

Schubert, B., Lee, J., Majidi, C. & Fearing, R. S. 2008 Sliding induced adhesion of stiff polymer microfiber arrays: 2. Microscale behaviour. *J. R. Soc. Interface* **5**, 845–853. (doi:10.1098/rsif.2007.1309)

Sethi, S., Ge, L., Ci, L., Ajayan, P. M. & Dhinojwala, A. 2008 Gecko-inspired carbon nanotube-based self-cleaning adhesives. *Nano Lett.* **8**, 822–825. (doi:10.1021/nl0727765)

Sills, S., Vorvolakos, K., Chaudhury, M. K. & Overney, R. M. 2007 Molecular origins of elastomeric friction. In *Fundamentals of friction and wear at the nanoscale* (eds E. Gnecco & E. Meyer). New York, NY: Springer.

Sitti, M. & Fearing, R. S. 2003 Synthetic gecko foot-hair micro/nano structures as dry adhesives. *J. Adh. Sci. Technol.* **17**, 1055–1073. (doi:10.1163/156856103322113788)

Sun, W., Neuzil, P., Kustandi, T. S., Oh, S. & Samper, V. D. 2005 The nature of the gecko lizard adhesive force. *Biophys. J.* **89**, L14–L17. (doi:10.1529/biophysj.105.065268)

Tambe, N. S. & Bhushan, B. 2005 Friction model for the velocity dependence of nanoscale friction. *Nanotechnology* **16**, 2309–2324. (doi:10.1088/0957-4484/16/10/054)

Tao, Z. & Bhushan, B. 2007 Velocity dependence and rest time effect on nanoscale friction of ultrathin films at high sliding velocities. *J. Vac. Sci. Technol. A* **25**, 1267–1274. (doi:10.1116/1.2435381)

Tian, Y., Pesika, N., Zeng, H., Rosenberg, K., Zhao, B., McGuiggan, P., Autumn, K. & Israelachvili, J. 2006 Adhesion and friction in gecko toe attachment and detachment. *Proc. Natl Acad. Sci. USA* **103**, 19 320–19 325. (doi:10.1073/pnas.0608841103)

Vajpayee, S., Long, R., Shen, L. L., Jagota, A. & Hui, C. Y. 2009 Effect of rate on adhesion and static friction of a film-terminated fibrillar interface. *Langmuir* **25**, 2765–2771. (doi:10.1021/la8033885)

Volterra, E. & Zachmanoglou, E. 1965 *Dynamics of vibrations*. Columbus, OH: Charles E. Merrill Books.

Vorvolakos, K. & Chaudhury, M. K. 2003 The effects of molecular weight and temperature on the kinetic friction of silicone rubbers. *Langmuir* **19**, 6778–6787. (doi:10.1021/la027061q)

Ward, I. M. & Sweeney, J. 2004 *An introduction to the mechanical properties of solid polymers*. Chichester, UK: John Wiley & Sons.

Williams, E. E. & Peterson, J. A. 1982 Convergent and alternative designs in the digital adhesive pads of scincid lizards. *Science* **215**, 1509–1511. (doi:10.1126/science.215.4539.1509)

Yamaguchi, T., Gravish, N., Autumn, K. & Creton, C. 2009 Microscopic modelling of the dynamics of frictional adhesion in the gecko attachment system. *J. Phys. Chem.* **113**, 3622–3628. (doi:10.1021/jp8067415)

Zhao, B. X., Pesika, N., Rosenberg, K., Tian, Y., Zeng, H. B., McGuiggan, P., Autumn, K. & Israelachvili, J. 2008 Adhesion and friction force coupling of gecko setal arrays: implications for structured adhesive surfaces. *Langmuir* **24**, 1517–1524. (doi:10.1021/la702126k)